COBEM 2023 27TH INTERNATIONAL CONGRESS OF MECHANICAL ENGENEERING

ABCM Brazilian Society of Mechanical Sciences and Engineering
27th ABCM International Congress of Mechanical Engineering
December 04-08, 2023, Florianópolis-SC, Brazil

COB-2023-1087
COMPUTATIONAL TOOL FOR PRELIMINARY EIGENVALUES ANALYSIS OF WIND TURBINE BLADES

Júlia da Silva Maschietto
Prof. Dr. Antônio Cândido Faleiros
julia.maschietto@aluno.ufabc.edu.br
antonio.faleiros@ufabc.edu.br

Prof. Dr. Juan Pablo Julca Avila
UFABC, 5001 Estados Avenue, Santo André, SP - 09210-580, Brazil.
juan.avila@ufabc.edu.br

Abstract. *There are currently high investments in the Brazilian and global wind sector, as in recent years the share of wind energy in the energy matrix has increased significantly. Consequently, wind turbines are widely studied. During the operation of wind turbines, the blade is subjected to high-speed winds, which can cause unwanted phenomena if the design is not considering bending and torsion vibrations. The objective of this work is to fill the research gap related to the scarcity of works that address the mathematical implementation using the Ritz-Galerkin method to solve the eigenvalues of wind turbine blades. The first version of a computational code was developed to determine the free vibration characteristics of a wind turbine blade with flexo torsional behavior. The wind turbine blade is modeled as an Euler-Bernoulli beam with a variable cross-section along its length. Hamilton's principle is used to derive the blade's equation of motion. The eigenvalues problem was solved analytically and numerically using the Assumed Modes Method and Ritz-Galerkin. The code elaborated in the Mathematica software produced results consistent with those in the literature for the first four natural frequencies and respective forms of modes.*

Keywords: *Wind turbine blade, Eigenvalue analysis, Galerkin's method, Euler beam model, Flexo-torsional coupling.*

1. INTRODUCTION

According to the Wind Electricity Monitoring Report made by the International Energy Agency, the generation of electricity from wind energy has been growing rapidly worldwide. In 2021 global wind energy production increased by 273 TWh, a growth of 55% higher than the previous year.

Studies carried out by the Brazilian Business Council for Sustainable Development show that Brazil has increased investment in technologies and the country has great potential for wind energy generation, CEBDS (2019). Today, this type of energy matrix corresponds to 10% of the total Brazilian matrix.

Wind turbines are equipment that converts wind energy into electrical energy. A wind turbine blade can undergo excessive flexural and torsional deformations during operation and may structurally fail, causing temporary or permanent deformations, impairing the operation of the wind turbine.

The dynamic response of the blade depends on its natural vibration characteristics given by the natural frequencies and modes of vibration. For a given natural frequency, there is a natural mode of vibration with flexo torsional coupling.

Regarding the bibliography, Dokumaci (1987) developed the exact solution of partial differential equations which govern the free vibration of a beam. In addition to the analytical methods, approximate methods were also used to solve the problem of free vibration of beams with flexotortional coupling. Two of them were used in this article, the Assumed Modes Method (AMM) and the Ritz-Galerkin Method.

Furthermore, L. Meirovitch (2001) studied several resolution methods for the coupled vibration problem. The method of Assumed Modes stands out, which consists of assuming a solution in the form of a sum of products of admissible functions, functions given by the modes of vibration, and generalized coordinates. Finally, the problem of eigenvalues is solved. Rao and Carnegie (1970) studied the flexo-torsion vibrations of a blade using Galerkin's method, they determined the natural frequencies and coupled modes of the blade.

During the design phase of a blade, it is necessary to know its natural frequencies and modes of vibration for two reasons, first, to stay away from the frequency range of cyclic loads induced by the wind of different speeds, that is, to stay away from the resonance zone, and also to conduct realistic dynamic analysis in the time domain. Thus arises the motivation of the present work to determine the natural characteristics of vibration through a computational code using the concepts presented in the bibliographies.

1.1 Configuration of wind turbines

In this work is considered the most common horizontal axis turbine (HAWTs) whose blades are connected on the horizontal axis as shown in Fig. (1(a)). In this figure, it is possible to observe the main structural components such as the tower, blades, and hub. The tower is the supporting structure of the wind turbine, blades are long and have an aerodynamic profile and are the focus of this research, as they are the main component of the turbine and suffer great structural stresses.

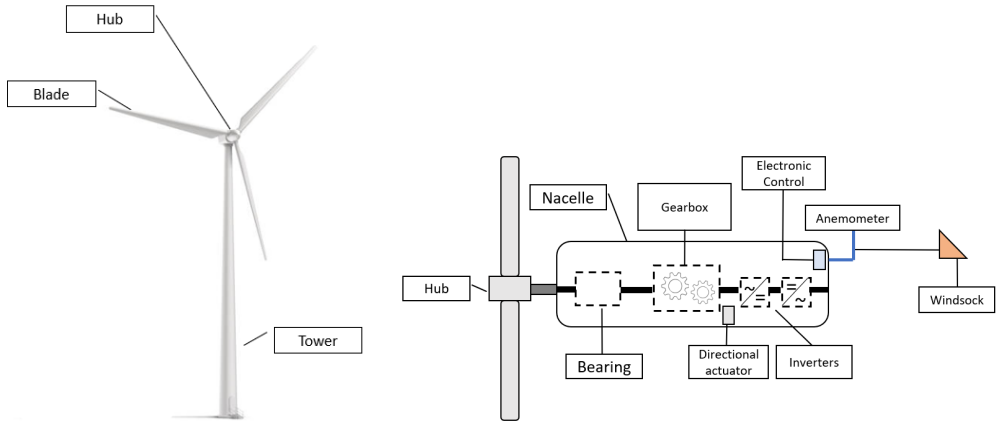

(a) HAWTs wind turbine (b) Diagram of a Nacelle - wind turbine. A self-made figure

Figure 1: Characterization of wind turbine components

Hub is the part responsible for joining the blades. The nacelle shown in Fig. (1(b)), is an important component that contains several wind turbine equipment such as electronic and hydraulic control systems, and transmission box, among others.

2. MATHEMATICAL MODELING

2.1 Blade characterization

The free vibration equations of the beam with flexo torsional deformations are developed, and considerations are made for the characterization of the wind blade.

1. The cross-section of the beam remains plane after deformation.
2. The beam has a length considerably greater than the other dimensions, such as its thickness.
3. The beam material is homogeneous and has a linear-elastic behavior.
4. Effects of rotational inertia and transverse shear strains are neglected.

The wind blade used in the modeling of this work is the CART turbine blade (Controls Advanced Research Turbine), a wind turbine located in Colorado. The CART turbine is an experimental platform for studying new control and power regulation systems. The material and geometric properties of the blade are public and are presented in Stol (2003). The table presented in the work by Stol (2003) provides data such as the polar radius of gyration r, the centroidal coordinate x_C, distance between the shear center and the centroid, r_x, the distribution of mass per unit length, μ, blade length, L, bending stiffness, EI, and torsional stiffness, GJ, data on moments of inertia of the blade cross-section per unit length around the axes x, I_x/L and z, I_z/L. The cross-section of the blade has a symmetry plane that coincides with the xy plane, as shown in Figure 2. This figure also illustrates the parameters used in this work. The origin of the coordinate system is fixed at the shear center.

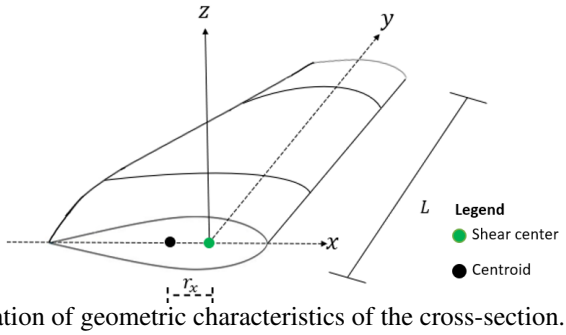

Figure 2: Representation of geometric characteristics of the cross-section. A self-made figure.

In the work of Stol (2003), the properties of the CART turbine wind blade are presented, that is, each section of the blade has a value for the previously mentioned parameters. In this article, the average properties of the blade will be used, so, in order to obtain them, the integration process was carried out and the results are shown in Tab.1

Table 1: Parameters of the blade object of study

Variable	L	μ	r_x	r	α	GJ_y	EI_x	I_x
Value	19.95	102.09	0.0901	0.363	1.061	1.090 $\times 10^7$	3.843 $\times 10^7$	2.784
Unit	[m]	[kg/m]	[m]	[m]	dimensionless	$[N.m^2]$	$[N.m^2]$	[Kg.m]

2.2 Blade deformation analysis

The blade suffers flexion and torsion deformations, in this way, its position in relation to its coordinate system changes with time. Four coordinate systems $[O, x, y, z]_0$, $[O, x, y, z]_1$, $[O, x, y, z]_2$ and $[O, x, y, z]_3$ are defined to describe the deformation of the blade, (Bastawrous, 2015). The global coordinate system $[O, x, y, z]_0$ is the fixed and inertial reference with its origin at O_0 fixed on the wind turbine rotor, as shown in Fig. (3(a)).

The coordinate system $[O, x, y, z]_1$ is fixed at the shear center of the blade root, with axis z_0 coinciding with z_1, in addition, the blade rotates around axis z_0 with constant angular velocity Ω and angle of rotation Ωt, Fig. (3(b)). It is worth mentioning that in this work, the blade does not rotate, so $\Omega t = 0$.

Let us consider a generic point P whose coordinates in the system $[O, x, y, z]_1$ are $h_1 = [xyz1]^T$, as we can see at Fig. (3(c)).

Another coordinate system used is $[O, x, y, z]_2$, which presents a distance y from the origin O_1 along the axis y_1, represented in Fig. (3(d)). This figure also shows a shear curve, formed after deformation, this curve represents the union of the shear centers of the cross sections of the blade.

The transformation matrix of the coordinate system from $[O, x, y, z]_1$ to $[O, x, y, z]_2$ is given by $T_{1\to2}$ bellow, according to equation (1), (Bastawrous, 2015)

$$T_{1\to2} = \begin{bmatrix} 1 & 0 & 0 & 0 \\ 0 & 1 & 0 & y \\ 0 & 0 & 1 & 0 \\ 0 & 0 & 0 & 1 \end{bmatrix} \begin{bmatrix} 1 & 0 & 0 & 0 \\ 0 & 1 & -w'(y,t) & y \\ 0 & w'(y,t) & 1 & w(y,t) \\ 0 & 0 & 0 & 1 \end{bmatrix} \tag{1}$$

Where $w(y, t)$ is the blade deflection at a given instant of time and $w'(y, t)$ is the derivative of $w(y, t)$ with respect to y.

A third coordinate system $[O, x, y, z]_3$ is introduced, so that its origin coincides with the origin of the second coordinate system $[O, x, y, z]_2$, that is $O_2 = O_3$. The coordinate transformation matrix from $[O, x, y, z]_2$ to $[O, x, y, z]_3$ is presented as Eq. (2). In this coordinate system, x_3 is rotated by the angle β of axis x_2 around y_2, Fig. (3(e)).

$$T_{2\to3} = \begin{bmatrix} 1 & 0 & \beta(y,t) & 0 \\ 0 & 1 & 0 & 0 \\ -\beta(y,t) & 0 & 1 & 0 \\ 0 & 0 & 0 & 1 \end{bmatrix} \tag{2}$$

The last coordinate transformation is given by the direct transformation of the coordinate system $[O, x, y, z]_1$ to $[O, x, y, z]_3$. Considering $T_{1\to3} = D_{1\to2}E_{1\to2}T_{2\to3}$, it is possible to write $T_{1\to3} = T_{1\to2}T_{2\to3}$. The expression $h_1 = T_{1\to3}h_3$ is used to write the position of P in relation to the reference frame $[O, x, y, z]_1$ after deformation. Where h_3 is the position of the point P after the torsion, represented by the vector $[x, y, z, 1]^T$. The blade does not warp after torsional deformation, and considering that the blade suffers small deformations. So, h_1 results in Eq. (3a). To define the velocity it is necessary to differentiate the vector (3a), then, the velocity vector is expressed as Eq. (3b)

$$h_1 = \begin{bmatrix} x + z\beta \\ y - zw' \\ z + w - x\beta \\ 1 \end{bmatrix} \tag{3a}$$

$$\dot{h_1} = \begin{bmatrix} z\dot{\beta} \\ -z\dot{w'} \\ \dot{w} - x\dot{\beta} \\ 0 \end{bmatrix} \tag{3b}$$

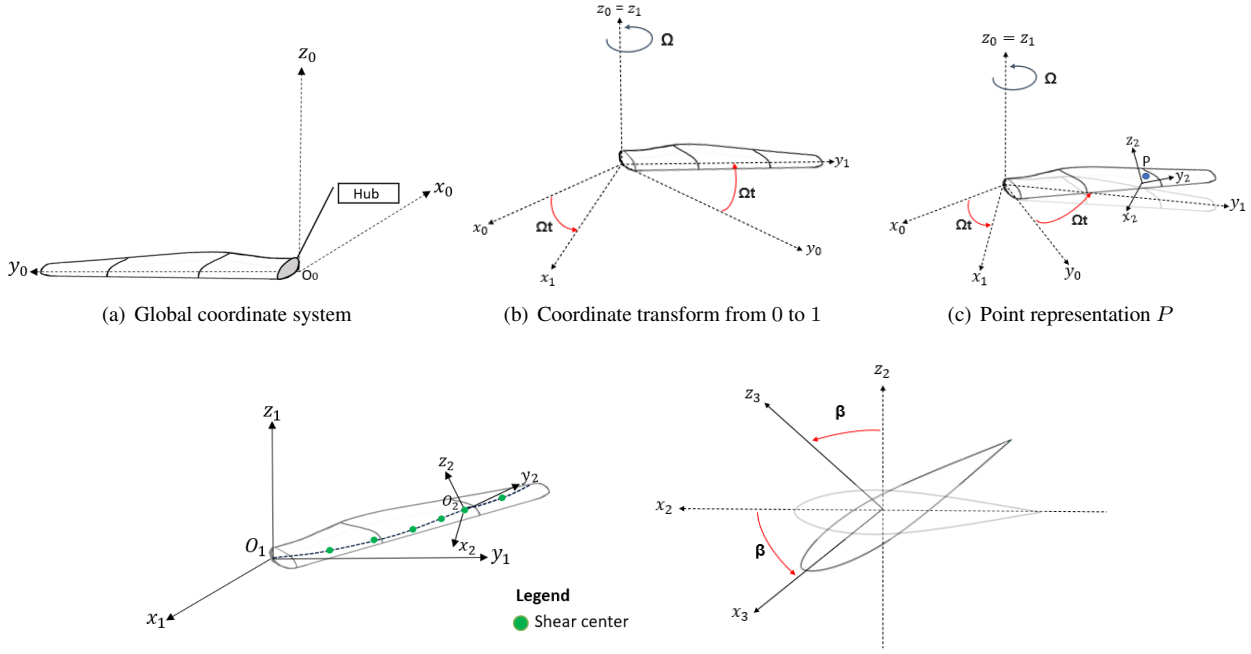

(a) Global coordinate system (b) Coordinate transform from 0 to 1 (c) Point representation P

(d) Coordinate transform from 1 to 2 (e) Cross-section of blade twisted by angle β

Figure 3: Blade position after coordinate transformations. Self-made figures

2.3 Modeling of the fixed and uniform blade

2.3.1 Potential Energy

Potential energy comes from elastic deformations. The work of the internal forces is integrated across the cross-sectional area and the potential energy per unit length is obtained. The strain energy density V_0 of an elastic material is given by Timoshenko and Goodier (1951)

$$V_0 = \int_0^{\epsilon_{yy}} E\epsilon_{yy}d\epsilon_{yy} + 2G(\int_0^{\epsilon_{xy}} \epsilon_{xy}d\epsilon_{xy} + \int_0^{\epsilon_{yx}} \epsilon_{yx}d\epsilon_{yx} + \int_0^{\epsilon_{yz}} \epsilon_{yz}d\epsilon_{yz} + \int_0^{\epsilon_{zy}} \epsilon_{zy}d\epsilon_{zy} + \int_0^{\epsilon_{zx}} \epsilon_{zx}d\epsilon_{zx} + \int_0^{\epsilon_{xz}} \epsilon_{xz}d\epsilon_{xz}) \tag{4}$$

where ϵ_{yy} is the normal deformation in the direction of the y axis. The notation ϵ_{ij} is used to define that the shear deformation acts in a plane perpendicular to the i axis and parallel to the j axis. The elastic deformation is expressed as

$$\begin{pmatrix} \epsilon_{yx} \\ \epsilon_{yy} \\ \epsilon_{yz} \end{pmatrix} = \begin{pmatrix} \frac{1}{2}z\beta'(y,t) \\ -zw''(y,t) \\ \frac{1}{2}x\beta'(y,t) \end{pmatrix} \tag{5}$$

For the development of the work it is considered that $\epsilon_{yx} = \epsilon_{xy}$, $\epsilon_{yz} = \epsilon_{zy}$, $\epsilon_{zx} = \epsilon_{xz}$. Substituting the Eq. (5) in the equation (4), the elastic potential energy per unit volume is obtained according to

$$V_0 = \frac{1}{2}Ez^2(w'')^2 + \frac{1}{2}G\beta'^2(z^2 + x^2) \tag{6}$$

where E is Young's elastic modulus and G is the shear rigidity modulus. The potential energy is integrated over the cross-sectional area to obtain the elastic potential energy per unit blade length. Integrating the Eq. (6) over the volume of the blade and doing the integral in a transversal section, we arrive to (Bastawrous, 2015)

$$V_0 = \int_0^L \left(\frac{1}{2}EI_{x_2}(w'')^2 + \frac{1}{2}GJ_{y_2}(\beta')^2\right) dy \tag{7}$$

2.3.2 Kinetic Energy

The kinetic energy of the blade is given by

$$T = \frac{1}{2}\int \rho\dot{h}\cdot\dot{h}\ dV = \frac{1}{2}\int_0^L \left(\int_A \rho\dot{h}\cdot\dot{h}\ dA\right) dy \tag{8}$$

where $\dot{h}$ is presented in the Eq. (3b). The dot product, $\dot{h} \cdot \dot{h}$, is developed to obtain the kinetic energy. The result is multiplied by ρ and integrated over a cross-section of the blade $\int_A \rho\, \dot{h} \cdot \dot{h}\ dA$,

$$\mu = \int_A \rho\, dA = \rho\, A, \quad \mu\, r^2 = \int_A \rho \left(\tilde{x}^2 + z^2\right) dA. \tag{9}$$

The constants that appear in the energy expression are $I_{x2m} = \int_A \rho z^2\, dA$, $J_{y2m} = \int_A \rho \left(x^2 + z^2\right)\, dA, J_{y2m} - I_{x2m} = \int_A \rho x^2\, dA, \int_A \tilde{x}\, dA = 0, \int_A z\, dA = \int_A \tilde{z}\, dA = 0, \int_A \rho x\, dA = r_x \mu$. The constant I_{x2m} is the mass moment of inertia per unit length about the axis x_2. Terms $J_{y2m}\dot{\beta}^2 - 2\mu r_x \dot{\beta}\dot{w} + I_{x2m}\dot{w}'^2 + \mu \dot{w}^2$ give the quadratic part of the blade's kinetic energy, Eq. (8)

Defining the polar radius of gyration r as $r^2 = \frac{1}{\mu}\int_A \rho \left(\tilde{x}^2 + z^2\right) dA$ and $J_{y2m} = \mu \left(r^2 + r_x^2\right)$ and replacing J_{y2m} in the Eq. (8), the expression of kinetic energy per unit length is given by,

$$T = \frac{1}{2}\int_0^L \left(\mu \dot{w}^2 - 2\mu r_x\, \dot{w}\, \dot{\beta} + \mu \left(r^2 + r_x^2\right) \dot{\beta}^2 + I_{x2m}(\dot{w}')^2\right)\, dy \tag{10}$$

2.3.3 Hamilton's Principle

Hamilton's principle was studied by Clough and Penzien (1993) and L. Meirovitch (2001). It is a variational principle, that is, it presents variations and virtual displacements, simplifying the problem for analytical mechanics, with the use of virtual displacements. The blade's governing equations come from Hamilton's Principle. The deductions of equations are presented in Bastawrous (2015). Equation (11) represents Hamilton's principle for the conservative motion of a particle, it considers the entire motion of the system between two instants t_1 and t_2, Leonard Meirovitch (1967).

$$\int_{t_1}^{t_2} (\delta T - \delta V_0) dt = 0 \tag{11}$$

where T is the kinetic energy and V_0 the potential energy at an instant of time. To apply Hamilton's Principle, the length integral change of the potential energy term was calculated and integrated by parts. After mathematical manipulations the following equation was obtained

$$\begin{aligned}\int_{t_1}^{t_2} (\delta T - \delta V_0) dt = \int_{t_1}^{t_2}\int_0^L (-\mu\ddot{w} + \mu r_x \ddot{\beta} + (I_{x2m}\ddot{w}')') - (EI_{x2}w'')'')\delta w + (\mu r_x \ddot{w} - J_{y2m}\ddot{\beta} + \\ (GJ_{y2}\beta')')\delta\beta dy dt + \int_{t_1}^{t_2} (-\int_0^L I_{x2m}\ddot{w}'\delta w - \int_0^L GJ_{y2}\beta'\delta\beta - \\ \int_0^L EI_{x2}w''\delta w' + (\int_0^L EI_{x2}w''\delta w) dt\end{aligned} \tag{12}$$

The system of partial differential equations of the blade vibrations are

$$-\mu\ddot{w} + \mu r_x \ddot{\beta} - (EI_{x2}w'')'' = 0\ , \qquad \mu r_x \ddot{w} - J_{y2m}\ddot{\beta} + (GJ_{y2}\beta')' = 0\ . \tag{13}$$

These are exactly the equations (1) and (2) of Dokumaci (1987).

Boundary conditions are required for the problem to be solved. For this study, the boundary conditions given by Mendelson and Gendler (1951) were used. There are six boundary conditions in all, including geometric and natural constraints, and they are

$$w(0,t) = 0, \quad \beta(0,t) = 0, \quad w'(0,t) = 0, \quad \beta'(L,t) = 0, \quad w''(L,t) = 0, \quad w'''(L,t) = 0 \tag{14}$$

The first two boundary conditions are geometric. The blade is wedged in the root, so the deflection $w(0,t) = 0$ and the twist angle $\beta(0,t) = 0$ in the wedge region are zero. The third boundary condition $w'(0,t) = 0$ indicates that the first derivative of the deflection, the slope, is equal to zero. Boundary condition $\beta'(L,t)$ concerns the torque, the first derivative of the torsion angle at the blade tip. The last two boundary conditions are the second and third derivatives of the deflection w, representing the blade bending moment and the shear force respectively.

3. SOLUTION METHODS

3.1 Exact solution

To find the vibration frequencies of the wind blade, it is represented as a uniform beam. Coupled flexo-torsional vibrations are observed when the shear center does not coincide with the centroid of the blade cross-section.

The governing equations related to free vibrations are the pair of coupled equations with constant coefficients (13), where t denotes time, and y is the elastic axis of the blade. To find exact solutions of this system of differential equations, Dokumaci (1987) note that it has a separable solution of the form

$$w(y,t) = W(y)q(t) \qquad \beta(y,t) = B(y)q(t) \tag{15}$$

where $W(y)$ and $B(y)$ depend only on the spatial coordinate y and $q(t) = \exp(j\omega t)$ depend only on time and the constant ω. Here j is the imaginary unit. This form of $q(t)$ correspond to an harmonic movement of frequency ω. Performing the substitution of these functions at the system of partial differential equations (13) we get, after dividing by $\exp(j\omega t)$

$$\left(D^4 - \lambda_w\right) W(y) - \lambda_w r_x B(y) = 0 \tag{16}$$

$$\left(D^2 + \alpha\lambda_\beta\right) B(y) + (r_x/r^2)\lambda_\beta W(y) = 0 \tag{17}$$

where the operator $D = L\, d/dy$, is the multiplication of L by the derivative in y. The dimensionless parameters λ_w, λ_β, α, are defined by

$$\lambda_w = \left(\frac{\mu L^4}{EI_{x2}}\right)\omega^2\,, \qquad \lambda_\beta = \left(\frac{\mu r^2 L^2}{GJ_{y2}}\right)\omega^2\,, \qquad \alpha = 1 + \left(\frac{r_x}{r}\right)^2 \tag{18}$$

Solving the system (16) and (17) for $W(y)$ and $B(y)$ we get

$$(D^6 + \alpha\lambda_\beta D^4 - \lambda_w D^2 - \lambda_w\lambda_\beta)W(y) \quad or \quad B(y) = 0 \tag{19}$$

who has solutions of the form $\exp(sy/L)$. The parameter s is a root of the characteristic equation

$$s^6 + \alpha\lambda_\beta\, s^4 - \lambda_w\, s^2 - \lambda_w\lambda_t = 0 \tag{20}$$

Dokumaci (1987) proved that, in the region of interest, $\alpha \geq 1$, this equation has six roots

$$s_1, \quad -s_1, \quad js_2, \quad -js_2, \quad js_3, \quad -js_3$$

where j is the imaginary unity. Since the system (16) and (17) are linear and homogeneous, a linear combination of solutions is another solution. We have a linear combination of six terms for $W(y)$ and another six for $B(y)$. Using the linearly independence of the functions involved, only six from these twelve constants are independent. As linear combinations of $\exp(jsz)$ and $\exp(-jsz)$ (z is any real number or real expression and j is the imaginary unit) can be written as a linear combination of $\sin(sz)$ and $\cos(sz)$ and linear combinations of $\exp(sz)$ and $\exp(-sz)$ can be written as a linear combination of $\sinh(sz)$ and $\cosh(sz)$, the solutions can be written in the form

$$\begin{aligned} W(y) &= A_1\cosh\left(\frac{s_1 y}{L}\right) + A_2\sinh\left(\frac{s_1 y}{L}\right) + A_3\cos\left(\frac{s_2 y}{L}\right) + A_4\sin\left(\frac{s_2 y}{L}\right) + \\ &\quad \frac{r^2(s_3^2 + \alpha\lambda_\beta)}{r_x\lambda_\beta}\left[B_5\cos\left(\frac{s_3 y}{L}\right) + B_6\sin\left(\frac{s_3 y}{L}\right)\right] \end{aligned} \tag{21}$$

$$\begin{aligned} B(y) &= \frac{\lambda_w - s_1^4}{r_x\lambda_w}\left[A_1\cosh\left(\frac{s_1 y}{L}\right) + A_2\sinh\left(\frac{s_1 y}{L}\right) + A_3\cos\left(\frac{s_2 y}{L}\right) + \right. \\ &\quad \left. A_4\sin\left(\frac{s_2 y}{L}\right)\right] + B_5\cos\left(\frac{s_3 y}{L}\right) + B_6\sin\left(\frac{s_3 y}{L}\right) \end{aligned} \tag{22}$$

Taking (21) and (22) into the boundary conditions given by (14), we get an homogeneous linear algebraic system for the constants A_i, and B_i. To get a nontrivial solution, the determinant of the coefficient matrix of this system has to be zero. The roots of this determinant gave us the frequency. Bellow we list the four lower frequencies in units of rad/s,

$$\omega_1 = 5.419\,, \qquad \omega_2 = 33.907\,, \qquad \omega_3 = 70.871\,, \qquad \omega_4 = 94.812\,. \tag{23}$$

Coupled flexo-torsional modes of vibration were obtained from the calculation of the functions $W(y)$ and $B(y)$ for each frequency, which are plotted in Figure 4, where the subscript i of $W(y)$ and $B(y)$ refers to the natural frequency w_i.

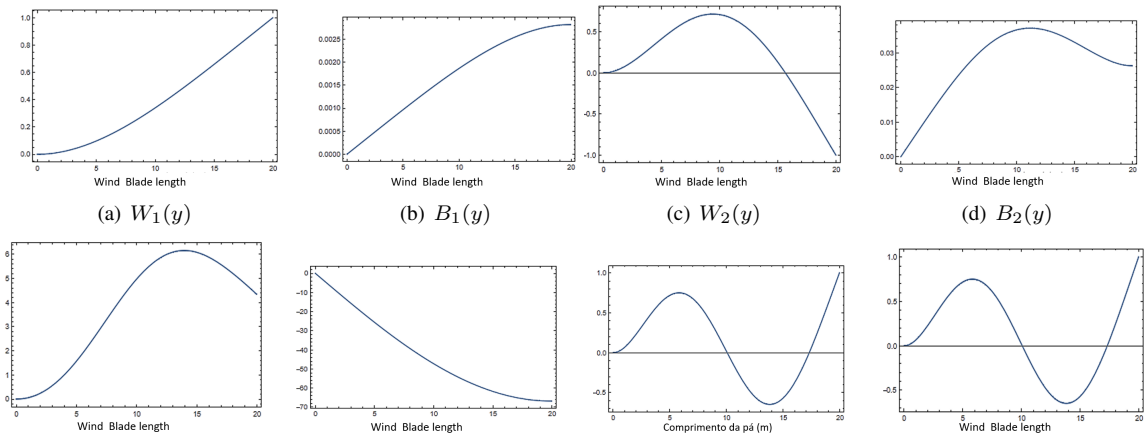

(a) $W_1(y)$ (b) $B_1(y)$ (c) $W_2(y)$ (d) $B_2(y)$

(e) $W_3(y)$ (f) $B_3(y)$ (g) $W_4(y)$ (h) $B_4(y)$

Figure 4: Bending and Twisting Modes - Exact Solution

3.2 Assumed Modes Method

The trial solution in the assumed modes method for bending and torsion respectively are

$$w(y,t) = \sum_{i=1}^{N} W_i(y) q_i(t) \qquad \beta(y,t) = \sum_{i=1}^{N} B_i(y) q_i(t) \tag{24}$$

The test functions $W_i(y)$ and $B_i(y)$ are the exact solutions for the case of a prismatic cantilever beam given by Dokumaci (1987) and $N = 4$. At this first moment, $q_i(t)$ are generalized coordinates, and with the approximate solution, this problem became one with a finite degree of freedom. Introducing (24) into the energy expressions (7) and (10), we arrived at

$$V_0 = \frac{1}{2} \sum_{i=1}^{N} \sum_{j=1}^{N} k_{ij}\, q_i q_j \quad \text{and} \quad T = \frac{1}{2} \sum_{i=1}^{N} \sum_{j=1}^{N} m_{ij}\, \dot{q}_i \dot{q}_j \tag{25}$$

The approximate solution (24) has to satisfy the Euler-Lagrange equations for conservative systems

$$\frac{d}{dt}\left(\frac{\partial L}{\partial \dot{q}_r}\right) - \frac{\partial L}{\partial q_r} = 0, \qquad r = 1, \ldots, N \tag{26}$$

where $L = T - V_0$ is the Lagrangian, with T and V_0 given by Eq. (7) and Eq. (10). Calculating the Lagrange equation with (25) we obtain

$$\sum_{i=1}^{N} m_{ri} \ddot{q}_i + \sum_{i=1}^{N} k_{ri} q_i = 0, \qquad r = 1, \ldots, N \tag{27}$$

This N scalar equalities lead us to a matrix equality

$$M\,\ddot{q} + K\,q = 0 \tag{28}$$

where q is the column matrix $q = [q_1 \cdots q_N]^T$, $M = (m_{ij})$ and $K = (k_{ij})$.

To determine the frequencies of vibrations, the generalized coordinate vector is written in the form $q = ae^{j\omega t}$, where j is the imaginary unit and $a = [a_1 \cdots a_n]^T$ is a constant column matrix with N rows. Substituting this expression in (28) and dividing by $\exp(j\omega t)$ we find

$$(K - \omega^2 M)\, a = 0 \tag{29}$$

This is an eigenvalue problem, whose solutions give the first N frequencies ω_i of vibration. Using the functions $W_i(y)$ and $T_i(y)$, $i = 1, \ldots, 4$ as trial functions, the matrix equation (29) is solved using Mathematica. The resulting frequencies are presented below

$$\omega_1 = 5.416\,, \qquad \omega_2 = 33.958\,, \qquad \omega_3 = 70.874\,, \qquad \omega_4 = 95.683\,. \tag{30}$$

3.3 Ritz-Galerkin method

The Ritz-Galerkin Method is used to obtain the coupled flexo-torsional vibration frequencies of the uniform cantilevered beam, in addition to the graphs of the modes of vibration. The system of ordinary differential equations of motion is given by Eq. (13) and the approximate solution will have the same form as that used in the exact solution, Eq. (15), with $q(t) = exp(j\omega t)$, were j is the imaginary unit. This mean that $W(y)$ and $B(y)$ has to be a solution of the system of equations defined by (16) and (17). Now the trial functions will be taken as the same form as that used by Rao and Carnegie (1970)

$$W(y) = \sum_{k=1}^{N} A_k\, f_k(y) \qquad B(y) = \sum_{k=1}^{N} B_k\, F_k(y) \tag{31}$$

where A_k and B_k are constant, $f_k(y)$ and $F_k(y)$ are defined by

$$f_k = \left(\frac{y}{L}\right)^{k+1} \left[\frac{(k+2)(k+3)}{6} - \frac{k(k+3)}{3}\left(\frac{y}{L}\right) + \frac{k(k+1)}{6}\left(\frac{y}{L}\right)^2\right], \quad F_k = \left(\frac{y}{L}\right)^{k} \left[1 - \frac{y}{k+1}\left(\frac{y}{L}\right)\right] \tag{32}$$

For the method to be efficient, the test functions must satisfy all the boundary conditions previously presented in Eq. (14) as, in fact, they do.

Functions (32) don't satisfy the equations (16) and (17). By the way, let us denote the left hand side of these equations by EOM1 and EOM2 that now will be written in the form EOM1 $= 0$ and EOM2 $= 0$. When the approximate solution (31) with functions f_k and F_k in (32) are substituted in the equations (16) and (17), the left hand side will not be zero. There will be residual errors. In the Ritz-Galerkin method, we assume that these errors are orthogonal to $f_k(y)$ and $F_k(y)$, with respect to the inner product

$$\langle g_1, g_2 \rangle = \int_0^L g_1(y)\, g_2(y)\, dy. \tag{33}$$

We specifically adopted

$$\int_0^L \text{EOM1}\, f_k(y)\, dy = 0 \quad \text{and} \quad \int_0^L \text{EOM2}\, F_k(y)\, dy = 0, \quad k = 1, \ldots, N \tag{34}$$

By performing the integrals and after mathematical manipulations we obtain

$$(K - \omega^2 M)X = 0. \tag{35}$$

This is an eigenvalue problem, whose eigenvalues provide ω^2, the square of the vibration frequencies. Eigenvalues are determined by $\det(K - \omega^2 M) = 0$. When they are replaced in the matrix equation (35), it is possible to determine the eigenvectors that, as we know, are not unique. We got them with the Eigensystem command in the Mathematica software. The obtained frequencies are

$$\omega_1 = 5.416\,, \qquad \omega_2 = 33.907\,, \qquad \omega_3 = 70.874\,, \qquad \omega_4 = 94.878\,. \tag{36}$$

and the mode shapes are shown in Fig. (5).

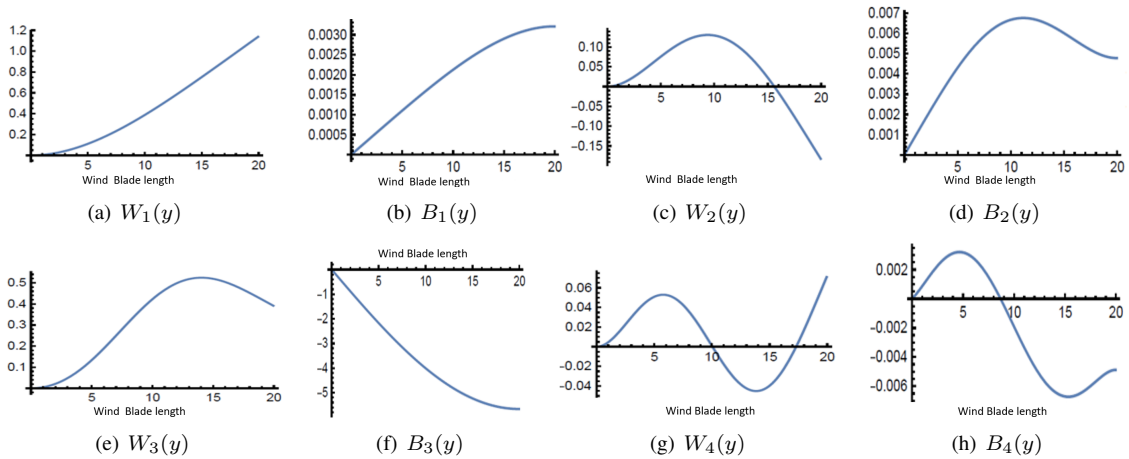

(a) $W_1(y)$ (b) $B_1(y)$ (c) $W_2(y)$ (d) $B_2(y)$

(e) $W_3(y)$ (f) $B_3(y)$ (g) $W_4(y)$ (h) $B_4(y)$

Figure 5: Bending and Twisting Modes - Assumed Modes Solution

3.4 Comparison of results

The values of the exact frequencies in rad/s were compared with the exact solution obtained in the reference Bastawrous (2015), Tab. (2) brings the results of the frequencies of the four coupled modes.

The frequencies obtained by the Ritz Galerkin Method were compared with those of the Assumed Modes.

Table 2: Comparison of blade frequencies using different methods

Method	Reference (rad/s) Bastawrous (2015)	Calculated (rad/s)
Exact Solution	5.544 ; 34.703 ; 63.442 ; 94.812	5.419 ; 33.907 ; 70.871 ; 94.812
MMA	5.424 ; 34.162, 70.874 ; 95.841	5.416 ; 33.958 ; 70.874 ; 95.683
Ritz-Galerkin	Not applicable	5.416; 33.907; 70.871; 94.878

The relative error, e_{rel}, between the bibliography values and the calculated for the exact solution is calculated using the next equation

$$e_{rel} = \frac{(f_{calc} - f_{ref})}{f_{ref}} \cdot 100\% \tag{37}$$

where f_{calc} is the frequency calculated from the approximate methods and f_{ref} is the result of the exact frequency.

In the exact solution, the third frequency is the one with the highest relative error, whose value found was 11.7% difference between the bibliographic reference and the calculated one. It is worth remembering that in the work of Bastawrous (2015) this value was omitted. For the Assumed Modes Method, the largest error of 0.59% is in the second frequency. Finally, in the Ritz-Galerkin method, the largest error is found in the fourth frequency, in the order of 1%. The results between the calculated methods,of the exact solution, as and approximate methods are shown in Tab. (3).

Table 3: Comparison of the results of calculated natural frequencies of the blade and approximate methods

Mode	Exact Solution (rad/s)	AMM (rad/s)	Galerkin (rad/s)
1	5.416	5.416	5.416
2	33.907	33.958	33.907
3	70.871	70.874	70.871
4	94.812	95.683	94.878

It is possible to notice that the frequencies of the approximate methods are equal or slightly higher than the exact ones, however, the results are satisfactory considering the error calculation procedure.

The largest relative error is that of the fourth frequency of the Assumed Modes Methods whose value is 0.9 %, less than 1%. In addition, the format of the modes obtained through the Exact and Galerkin Solutions have very similar results.

4. CONCLUSION

The main objective of this article was to conduct a study in order to find the coupled vibration frequencies and vibration modes of a uniform wind blade. The greatest contribution was the development of codes that can be easily reproduced and increased over time in other studies.

The results of the vibrating modes are similar to the methods used, increasing the robustness of the analyses. Exact solution studied uses the Dokumaci Method as a form of resolution for the flexo-torsional frequencies and modes of vibration, the Assumed Modes Method and Ritz-Galerkin were also used.

For future work, it is possible to add rotational movement to the problem, as well as increase the analyzes with a 3D model in FEM software.

5. ACKNOWLEDGEMENTS

We would like to thank the Coordination for the Improvement of Higher Education Personnel (CAPES) and the Graduate Program in Mechanical Engineering at the Federal University of ABC (UFABC) for their support.

6. REFERENCES

Bastawrous, Mary (2015). Structural Dynamic Modeling of Wind Turbine Blades. doi: 10.33140/RG.2.1.1965.9683.

CEBDS (2019). Você conhece as Fazendas de vento? url: https://cebds.org/voce-conhece-as-fazendas-de-vento/.Y0Wj-nbMLIU.

Clough, R.W. e J. Penzien (1993). Dynamics of Structures. Civil engineering series. McGraw-Hill. isbn: 9780071132411.

Dokumaci, E. (1987). “An exact solution for coupled bending and torsion vibrations of uniform beams having single cross-sectional symmetry”. pp. 443–449. doi: https://doi.org/10.3016/0022-460X(87)90408-1.

Meirovitch, L. (2001). Fundamentals of Vibrations. McGraw-Hill higher education. McGraw-Hill. isbn: 9780070413450.

Meirovitch, Leonard (1967). Analytical Methods in Vibrations. MACMILLAN COMPANY. isbn: 9780023801402.

Mendelson, Alexander e Selwyn Gendler (1951). “Analytical determination of coupled bending-torsion vibrations of cantilever beams by means of station functions”. University of North Texas Libraries, UNT Digital Library, p. 25. issn: 0022-460X.

Rao e W. Carnegie (1970). “Solution of the equations of motion of coupled-bending bending torsion vibrations of turbine blades by the method of ritz-galerkin”. International Journal of Mechanical Sciences 12.10, pp. 875–882. issn: 0020-7403.

Stol, Karl (jan. de 2003). “Geometry and Structural Properties for the Controls Ad- vanced Research Turbine (CART) from Model Tuning: August 25, 2003November 30, 2003”

Timoshenko, S. e J.N. Goodier (1951). "Theory of Elasticity". 2ª ed. McGraw-Hill Book Company.

7. RESPONSIBILITY NOTICE

The authors are solely responsible for the printed material included in this paper.